Reduction Midpoint Potentials of Bifurcating Electron Transfer Flavoproteins

A.-F. Miller, H. D. Duan, T. A. Varner and N. M. Raseek

Department of Chemistry, University of Kentucky, 505 Rose Street, Lexington KY 40506-0055

Abstract

Recently, a variety of enzymes have been found to accept electrons from NAD(P)H yet reduce lower-potential carriers such as ferredoxin and flavodoxin semiquinone, in apparent violation of thermodynamics. The reaction is favorable overall, however, because these enzymes couple the foregoing endergonic one-electron transfer to exergonic transfer of the other electron from each NAD(P)H, in a process called 'flavin-based electron bifurcation'. The reduction midpoint potentials (*E*°s) of the multiple flavins in these enzymes are critical to their mechanisms. We describe methods we have found to be useful for measuring each of the *E*°s of each of the flavins in bifurcating electron transfer flavoproteins.

Keywords

Flavin, Spectroelectrochemistry, Reduction midpoint potential, Electron bifurcation, Electron transfer flavoprotein.

1 Introduction to flavin-based bifurcation

1.1- Redox considerations

Some of life's most demanding reactions require extremely potent reductants, for example reduction of N_2 to NH_3. Indeed, a plethora of reactions at the core of anaerobic metabolism occur at very low reduction midpoint potentials ($E°$s) corresponding to strong reductants. However a ubiquitous currency for redox biochemistry is NAD(P)H, which is less reducing (higher-$E°$) and therefore incapable of supplying electrons for these reactions. In addition, several anaerobic processes display higher metabolic efficiency than can be accounted for by consideration of only low-potential electron donors for low-potential reactions (Buckel and Thauer, 2013). Enter electron transfer bifurcation ('bifurcation').

Figure 1 here.

Bifurcation employs a strongly exergonic transfer of one electron from NAD(P)H to drive endergonic transfer of the other electron to yield a more potent reductant (Herrmann et al., 2008). These enzymes thus trade quantity (two electrons from NAD(P)H) for quality (one more potent reducing equivalent, Figure 1). A variety of different overall reactions have been found to incorporate bifurcation to conserve excess energy in the form of potent reductants. The reverse reaction: confurcation, has been found to maximize the energy economy of multi-electron reactions by obtaining half the electrons needed from less potent reductants while drawing on powerful reducing equivalents only as needed to achieve overall thermodynamic favorability.

A particularly well-understood example is that of NADPH-dependent NAD reductase, Nfn, in which a combination of crystallography and spectroscopy have

revealed that a pair of electrons are transferred from NADPH to one of two flavins (Demmer et al., 2015; Lubner et al., 2017). This flavin transfers one electron to a Fe_2S_2 cluster which in turn reduces a second flavin (A_{ex} path in Figure 1), leaving the first one in a highly-energetic anionic semiquinone state (ASQ). The latter possesses sufficient driving force to reduce the first of a pair of Fe_4S_4 clusters that rapidly convey the electron to ferredoxin, at ≈ -400 mV (A_{end} path in Figure 1). A second round of similar electron transfer results in a second electron being passed to the second flavin, which then reduces NAD^+ at a higher-potential due to its status as the majority species in the NAD^+/NADH pool, in contrast to NADPH which acts as a low-*E*° donor due to a ten-fold excess of NADPH over $NADP^+$ (Buckel and Thauer, 2013). Thus, consumption of 2 NADPH effects reduction of one NAD^+ at higher *E*° and two Fd at lower *E*°. Although the first flavin acquires electrons as a pair, it donates them individually to two different acceptors, such that the path of electron transfer bifurcates at this flavin, the so-called 'bifurcation site'.

More and more enzymes are being found that perform bifurcating electron transfer from NAD(P)H. So far, all have been found to contain at least one flavin. Thus, use of a flavin as the site of bifurcation upon electron acceptance from NAD(P)H may be a unifying theme, and Buckel and Thauer have popularized the term 'flavin-based electron bifurcation', that explicitly distinguishes it from the earlier example of quinone-based electron bifurcation (Buckel and Thauer, 2013).

Electron bifurcation was first recognized as the Q-cycle in respiratory complex III (cytochrome bc_1 complex) where pairs of electrons are acquired by a quinone and bifurcated to the Rieske Fe_2S_2 cluster and cytochrome b_L. Energy is stored by

augmentation of the transmembrane proton gradient and one of the two electrons retains a lower $E°$ than the initial pair and therefore can contribute half the reducing equivalents needed for another round (Buckel and Thauer, 2013; Zhu et al., 2007). Quinones are well suited to this role by their ready acceptance of pairs of electrons, but formation of a high-energy one-electron reduced intermediate which retains much of the energy from the exergonic electron transfer to the Rieske Fe_2S_2 cluster. From an electrochemical standpoint, we say that the semiquinone state is thermodynamically unfavorable ("thermodynamically suppressed"). Suppression of the semiquinone state has been proposed to be essential for bifurcation activity (Nitschke and Russell, 2012).

The extent to which a semiquinone state is suppressed is a continuum. Because it is intermediate in degree of reduction between the oxidized (OX) and two-electron reduced hydroquinone (HQ) states, the semiquinone state (SQ) will be maximally populated at a potential half-way between the $E°$s of reduction of OX to SQ ($E°_{OX/SQ}$) and of reduction of SQ to HQ ($E°_{SQ/HQ}$). At this potential, one can show that the formation constant of SQ, $K = [SQ]^2/[OX][HQ]$ is related to the two $1e^-$ $E°$s by $log(K) = (E°_{OX/SQ} - E°_{SQ/HQ})/59\ mV$ (Clark, 1960) pg 186. Thus, when $E°_{SQ/HQ}$ is more positive than $E°_{OX/SQ}$ we say that the two potentials are crossed, and less than half the population can adopt the SQ state in equilibrium with OX and HQ. For the example of $1e^-$ E°s crossed by 120 mV, $(E°_{OX/SQ} - E°_{SQ/HQ}) = -120\ mV$, SQ will constitute only 5% of the population when [OX]=[HQ] at $E°_{OX/HQ}$, and the free energy of the SQ will be 5.7 kJ/mol higher than either OX or HQ.

All enzymes known so far to bifurcate electrons from NAD(P)H possess at least one flavin, which therefore has been suggested to be the site of bifurcation. The flavin is

inherently well-suited to bifurcation, poised by its intrinsic *E*°s at a cusp between one-electron ($1e^-$) and two-electron ($2e^-$) redox reactivity. The *E*°s of free flavin mononucleotide (FMN) are $E°_{OX/SQ}$ = -313 mV and $E°_{SQ/HQ}$ = -101 mV (Anderson, 1983; Mayhew, 1999a), crossed by 212 mV, causing population of SQ to a maximum of ≈ 1% at neutral pH (Ehrenberg et al., 1967). The SQ is nonetheless energetically accessible via mechanisms employed in proteins to tune flavin *E*°s, as evidenced by the stable SQ of flavodoxin (Mayhew et al., 1969). However in other enzymes analogous non-covalent interactions suffice to diminish maximum SQ population well below the 0.01% level (Koder et al., 2002) and give this state the status of a transient high-energy intermediate, akin to a transition state. Thus, electrochemical characterization of flavin sites can shed light on whether they may be competent to execute bifurcation by virtue of suppressed SQ states, provided supportive kinetics also apply (Zhang et al., 2017).

1.2- Multiplicity of pathways and carriers

Electron bifurcation can be understood to couple two electron transfer events such that the exergonic transfer in-essence pays for the endergonic one (Figure 1, (Buckel and Thauer, 2018)). A second implication is that the bifurcation-competent enzyme must contain at least three redox-active cofactors: the bifurcation site, the higher-*E*° acceptor and the lower-*E*° acceptor (green, yellow and orange, respectively, in Figure 1). Titrations aiming to measure *E*°s of such systems will therefore have to parse the contributions of multiple sites. This is not only a spectral deconvolution challenge, but the fact that an *E*° measurement by definition addresses a system at equilibrium limits such measurements to descriptions of systems in which each cofactor's *E*° is measured in the presence of the reduced states of all higher-*E*° cofactors. Hence the system may

not necessarily be in the same state as that prevailing under turnover, wherein the paths and kinetics of electron transfer can produce intermediates in which a lower-*E*° cofactor is reduced in the presence of oxidized states of higher-*E*° cofactors (Hirst, 2010). Thus, a full mechanistic description of bifurcating enzymes must include elucidation of the paths and kinetics of electron transfer in addition to the *E*°s of the carriers, and it is desirable to measure *E*°s for individual cofactors in the presence of different mechanistically relevant states of the others (Sevrioukova et al., 1996). The work is advancing, but these and other critical measurements remain open opportunities to be addressed.

A consequence of bifurcation's employment of multiple paths of electron transfer is that there is in-principle the possibility that the proposed high-energy (strongly-reducing) SQ state could lose its electron via the exergonic path used to generate it. Thus, a gating mechanism is believed to be required, that would limit the exergonic path to acceptance of only one electron per pair from NADH, essentially shutting this path to the second and thus forcing it to employ the other, less favorable one.

Kinetics can play a critical role, for example if the path to the low-*E*° acceptor is very efficient (short) it can compete effectively even with a more favorable path that is slower. Moreover bifurcating electron transfer flavoproteins have been found to adopt multiple conformations that produce very different inter-cofactor differences, so it is proposed that conformational changes gate electron transfer (Demmer et al., 2017). Since conformational change can also affect *E*°s, one would like to assess the extent to which the *E*°s of each cofactor depend on the status of the others including redox state, conformational state and presence of bound substrate or product. Overall,

measurement of *E*°s, in conjunction with kinetics and course of electron transfer, are needed for a basic description of the mechanism of bifurcation, and knowledge of the *E*°s' dependence on events throughout the system will provide an invaluable picture of how the steps involved in bifurcation are coordinated and coupled. In what follows, we describe experiments and strategies we have employed to measure $1e^-$ and $2e^-$ *E*°s in an emerging group of bifurcating enzymes with diverse metabolic roles: the bifurcating electron transfer flavoproteins (Bf-ETFs).

ETFs in general have been known for a long time as the heterodimeric proteins that convey $1e^-$ equivalents between fatty acyl-CoA dehydrogenases and the respiratory quinone pool in mitochondria (Watmough and Frerman, 2010). These group-1 ETFs employ a single bound FAD cycling between its OX and ASQ states to execute the redox role, but the protein also contains a bound AMP which is required for protein folding, FAD incorporation and stability (Sato et al., 1993). Recently members of group-2 of the ETF family have been found to possess a second FAD in place of the AMP (Sato et al., 2003). Members of this family have also been shown to have bifurcating activity in combination with partner enzymes able to pass electrons to a higher-*E*° acceptor (Chowdhury et al., 2015; Chowdhury et al., 2014; Ledbetter et al., 2017). The Bf-ETF associated with nitrogen fixation in *Azotobacter vinelandii* acquired the name FixAB due to its metabolic role, but we refer to it as ETF here in accordance with its phylogenetics in the ETF family (note however that the A,B nomenclature of the two constituent proteins is reversed in Fix notation from its use among ETFs where 'A' denotes the larger protein of the two) (Garcia Costas et al., 2017). The nitrogen fixation-associated ETFs display genetic context that is common beyond diazotrophs, with a

gene for a putative ETF-quinone oxidoreductase (ETF-QR, = FixC) and a Fe_4S_4 protein (FixX) annotated as a *fixABCX* cluster, even in non-diazotrophs (Figure 2).

In FixABCX of *A. vinelandii*, NADH reduces a Bf-FAD bound in the AB dimer that is the ETF portion of the complex (Figure 2). One electron is believed to pass via the ETF's ET-FAD to the higher-*E*° ETF-QR component of the complex (product of *fixC*) while the other electron passes via FixX' Fe_4S_4 to ferredoxin (Fd) or flavodoxin (Fld) SQ (Ledbetter et al., 2017). An analogous mechanism is proposed for the Bf-ETF of *Acidaminococcus fermentans* which forms a complex with a co-expressed butyryl-CoA dehydrogenase that functions in the direction of reducing crotonyl-CoA to butyryl-CoA using a bound FAD (Chowdhury et al., 2014). After two iterations, the net reaction is 2 NADH + 2 Fd_{ox} + crotonyl-CoA → 2 NAD^+ + 2 Fd_{red} + butyryl-CoA (Herrmann et al., 2008).

Figure 2 here.

Among the Bf-ETF-associated complexes, *E*°s have been measured for the ETF of *Megasphaera elsdenii*, that displays bifurcating activity in conjunction with butyryl-CoA dehydrogenase (Sato et al., 2013). More recently, we have measured *E*°s for the ETF of FixABCX of *Rhodopseudomonas palustris* (Duan et al., 2018). In both cases, one flavin executes sequential $1e^-$ acquisitions at potentials of $E°'_{ASQ/HQ}$ = -136 mV and -83 mV (*M. elsdenii* and *R. palustris*, respectively) whereas the other flavin displays $2e^-$ reactivity at a lower potential compatible with oxidation of NADH ($E°'_{OX/HQ}$ =-279 mV and -223 mV *M. elsdenii* and *R. palustris*, respectively (Duan et al., 2018; Sato et al., 2013)). These values are consistent with the model, and the former higher-*E*° flavin with $1e^-$ activity is understood to be the ET-FAD while the lower-*E*° $2e^-$ flavin is suited to the role of Bf-

FAD. Crucially, the high $E°_{OX/ASQ}$s of +81 and -47 mV for the ET-flavin provide the insight that this FAD most likely rests in the ASQ state *in vivo*, and therefore would only be capable of accepting one electron from the Bf-FAD. Thus the protein has tuned this FAD's *E°*s to preclude passage of both electrons via the exergonic path, and the redox tuning thus enforces bifurcation, in these systems (although conformational gating may also occur). This illustrates the insights provided by E° values, in understanding bifurcation.

2 Theory associated with measurement of E°s

2.1- One- and two-electron redox reactions

The reduction midpoint potential *E°* is a statement of the free energy change per electron, for a reductive reaction:

$Ox + n\ e^- \rightarrow Red^-, \qquad E° = \frac{-1}{nF}\Delta G°$ (1)

where *n* is the number of electrons involved in the reductive reaction, Ox is the oxidized species (could be OX or one of the SQ states, for flavins), *Red* is the reduced species to which it is converted (could be a SQ or HQ state for flavins) and *F* is Faraday's constant.

Because *ΔG°* is in turn related to the equilibrium constant K_{eq}

$$E° = \frac{RT}{nF} ln\left(K_{eq}\right) \quad (2)$$

and we have that at an arbitrary potential *E* (vs. NHE), the concentrations of the Ox and Red species are related as follows:

$$E = E° + \frac{RT}{nF} ln\left(\frac{[Ox]}{[Red}\right) = E° + \frac{2.303RT}{nF} log\left(\frac{[Ox]}{[Red}\right) \quad (3),$$

which is the Nernst equation. At 'room temperature' (25 °C) *RT/F* = 25.7 mV. Thus plots of fraction reduced vs. *E-E°* show that 90% of the population will be reduced at a potential 60 mV below the *E°* whereas 90% of the population will be oxidized at a potential 60 mV above *E°* (Figure 3A). Thus measurements of the concentrations of *Ox* and *Red* species within the range of *E°*±60 mV avoid the difficulty of evaluating minute concentrations or small deviations from 100%. Since *E°* is generally not known in advance, this means that the first order of business will be some exploratory titrations designed to survey a promising range of *E*, and most determinations involve multiple attempts with multiple different indicator dyes as part of identifying an optimal range and a dye that does not interfere or interact with the enzyme. These preliminary experiments also serve to establish the nature of the reaction, as the slope of the plot of *log([Ox]/[Red]) vs. E* depends on *n*, the number of electrons, as n * *(F/*2.303*RT*) (Equation 3 and Figure 3B).

Figure 3 here.

2.2- Equilibrium between the flavin and an indicator dye

For cases where a redox indicator dye (*D*) is present at equilibrium with the flavin (*F*), the Nernst equation holds for both of them, and one can write that

$$E = E°_D + \frac{RT}{n_D F} ln\left(\frac{[D_{Ox}]}{[D_{Red}]}\right) = E°_F + \frac{RT}{n_F F} ln\left(\frac{[F_{Ox}]}{[F_{Red}]}\right) \quad (4)$$

thus

$$ln\left(\frac{[F_{Ox}]}{[F_{Red}]}\right) = \frac{n_F}{n_D} ln\left(\frac{[D_{Ox}]}{[D_{Red}]}\right) + \frac{F n_F}{RT}(E°_D - E°_F) \quad (5)$$

and a plot of $ln([F_{Ox}]/[F_{Red}])$ *vs.* $ln([D_{Ox}]/[D_{Red}])$ is expected to produce a straight line of slope n_F/n_D of 2, 1 or 0.5 depending on the reactions undergone by the flavin and the dye (F stands for flavin and D stands for indicator dye). The $E°_F$ is determined from the

value of $ln([F_{Ox}]/[F_{Red}])$ and the known $E°$ of the dye, $E°_D$, at the point at which $ln([D_{Ox}]/[D_{Red}])$ =0 (Massey, 1991). This point is in-essence the Y-intercept of the plot and equal to n_F $(F/RT)(E°_D - E°_F)$.

2.3- Effect of pH when proton acquisition is coupled to reduction

While reduction of OX to ASQ is described by equation 1 with n=1, reduction of OX to NSQ (neutral semiquinone), as in flavodoxin or FixC, requires consideration of uptake of a proton as well. In this case the reaction becomes

$Ox + e^- + H^+ \rightarrow RedH$

and one can show (Dutton, 1978) that

$$E°_{(pH)} = E°_{lim\ low\ pH} - 59\ mV\ log\frac{([H^+]+K_{Ox})}{([H^+]+K_{Red})} \qquad (6)$$

where K_{Ox} and K_{Red} are the acid dissociation constants of the Ox and Red species, and $E°_{lim\ low\ pH}$ indicates the $E°$ relating the protonated version of the Ox state to the protonated version of the Red state (the NSQ that is protonated at N5). In practice, OX is not protonated at pHs above 2, and even below pH 2, model flavins are protonated at N1, so this limiting value is not measured under physiological circumstances. However given that the pK of NSQ of flavodoxin is above 10 (O'Farrel et al., 1998), but the pK of OX is much lower than 4, most experimental determinations occur at pKs between the two where $K_{Ox} > [H^+] > K_{Red}$

$$E°_{(pH)} \approx E°_{lim\ low\ pH} - 59\ mV\ log\frac{(K_{Ox})}{[H^+]} \qquad (7)$$

and the observed $E°$ is expected to decrease by 59 mV for every unit increase in pH (Figure 4).

Figure 4 here.

For the case of $2e^-$ reduction of OX to anionic HQ^- that is associated with one H^+ per $2e^-$, analogous algebra shows that a 30 mV decrease in $E°$ is expected per unit increase in measurement pH. Since many enzymes are not maximally stable or soluble at pH 7.0, the same equations can be used to calculate the potentials of the dyes to be used at the pH of use from tabulated values (Duan et al., 2018). Before doing so, one must look up the pKs of the dye in both its reduced and oxidized form in order to learn how many protons, if any, must be accounted for. Excellent reference data can be found in (Clark, 1960; Ottaway, 1972).

3 Basic overview of a measurement

In general, an electrode is used to measure the ambient reductive potential *E* relative to the normal hydrogen electrode (NHE), and the natures and populations of the oxidized (Ox) and reduced (Red) states related by the $E°$ are revealed by spectroscopy after each of a series of stepwise partial reductions (Dutton, 1978). However, it is also convenient to employ a dye with an $E°$ near that of the sample as a mediator *cum* E indicator (within 30 mV is recommended (Massey, 1991)). This can be combined with slow continuous enzymatic delivery of reducing equivalents, to obtain a very stable self-contained experiment that yields excellent results (Massey, 1991). The flavin community has a history of both methods, and electrode-monitored measurements have been reviewed(Byron et al., 1989; Mayhew, 1999b). Therefore this treatise will concentrate on use of enzyme-delivered reducing equivalents and dye-based monitoring of the ambient E, because this method provides a very stable experiment that runs on its own, even overnight, once launched.

The challenge is to identify a dye whose optical signal does not overly complicate determinations of the population of flavin in its Ox and Red states. Some of our favorites are listed in Table 1. We highly recommend conducting the experiment in an inert atmosphere (recall that some glove boxes include H_2 in the atmosphere, which is not necessarily inert, depending on the enzymes and cofactors present). If a glove box or anaerobic chamber is available that is ideal, however skilled use of a gas train with O_2-depleted Ar (≤ 2 ppb) and high-quality gas-tight glassware can also yield excellent data sets.

Ideally, 'pure spectra' corresponding to the fully Ox and fully Red sample should be in hand (along with analogous spectra of the indicator dye), obtained at potentials more than 120 mV above and below the $E°$, respectively. These make it straightforward to deconvolute spectra containing mixtures of all four species, to extract their amplitudes at each point in the titration. Measurements of the populations (or concentrations) of Ox and Red should be made when these are at equilibrium with one-another, at each of several different values of E within 60 mV of $E°$. Emphasizing data obtained within 60 mV of $E°$ optimizes the accuracy with which populations are quantified, as neither Ox nor Red represents less than 10% of the total concentration within this range. (Analogous considerations apply for the dye, producing the recommendation that the $E°$ of the dye be within 30 mV of that of the sample, ideally). Samples should be sufficiently concentrated that at least one of Ox or Red can be quantified to better than ± 10% when present at only 10% of the population. Determinations should be made only after the populations have stabilized after each addition of titrant, in order to avoid confounding the measurement with kinetic effects. Moreover, the enzyme's cofactors must have

reached equilibrium with the indicator dye (or eletrode) reporting the solution *E*. To aid in this, a redox mediator should be included in the solution (Dutton, 1978). The indicator dye plays the same role as buffers do for pH, and the mediator catalyzes any needed interconversion of $1e^-$ and $2e^-$ reactions that may be necessitated by the use of a dye or enzyme with $2e^-$ reactivity, in conjunction with a $1e^-$ reductant. The goal is to establish a single redox equilibrium encompassing the solution, the sample and the electrode.

Data collected at several values of *E* are analyzed collectively by plotting ln([Ox]/[Red]) vs. *E*, or equivalently ln(fraction Ox/fraction Red) vs *E*. When only one of the two is measured directly (for example Ox) the other is calculated from the total concentration or (fraction Red) = 1-(fraction Ox). According to the Nernst equation (3) a straight line is predicted providing an excellent test of applicability of the model. An integer value is expected for n, and may be predicted from the spectra obtained. For the example of a flavin site in the OX state, observation of the spectral signature of ASQ upon reduction indicates that n=1 so a slope ≠ *RT/F* would reveal a need to improve the experiment. Assuming a straight line with a slope within 10% of that expected for the value of n, the value of *E* when ln([Ox]/[Red]) = 0 is the experimental value of *E*° (*E*-*E*°)=0 in Figure 3B)

4 Protocol for E° determination using xanthine/xanthine oxidase to deliver reducing equivalents.

4.1- Small apparatus and reagents: have these in the anaerobic chamber

- 2.0 mL cryovials
- 20 mL scintillation vials
- Precision Seal rubber septa

- Precision Glide needles
- Syringe filters (optional)
- Aluminum foil
- 500 µL self-masking cuvettes
- Micro stirring bars and a larger one to aid in retrieving them.
- Milli-Q water and Kimwipes
- Gel filtration mini-columns for switching buffers/removing dyes/testing for flavin dissociation.
- Set of pipetmen
- Buffer of your choice. (Note that if your normal buffers contain redox-supplements such as dithiothreitol, β-mercaptoethanol or TCEP (Tris(2-carboxyethyl)phosphine hydrochloride) you should determine in advance whether these interact with the indicator dyes, or react in the course of the titration. It is best to avoid possible complications.). It is wise to place some extra buffer and deionized water into the chamber the night before use, and allow to equilibrate with the inert atmosphere. These can permit rinsing of small apparatus and mid-course corrections.

4.2- Major instrumentation present in the anaerobic chamber

- Ecotherm chilling dry bath with lid, for keeping samples refrigerated.
- Spectrophotometer (associated computer is outside the chamber)

4.3- Reagents to prepare on the day of the titration, and use when fresh

- 1 µM stock solution of xanthine oxidase in the same buffer of your choice

- 500 µM xanthine in the same buffer of your choice. Xanthine does not dissolve easily in neutral pH. When preparing a more concentrated stock solution, 1-2 µL of 10 N NaOH may be added to 1 mL buffer to aid dissolution. After dilution to the desired working concentration, check the pH.
- 100 µM methyl viologen in the same buffer of your choice
- Dithionite for a stock solution. Weigh out powder into a vial and degas, prior to transfer into chamber, but dissolve by addition of desired volume of alkaline buffer only at time of use, inside the chamber (eg. to confirm a reduction end-point).
- Reference dyes in the same buffer of your choice. (Note that some dyes are sparingly soluble in water, and may need to be prepared as stock solutions in ethanol.)
- The enzyme to be characterized, in the buffer of choice.

4.4- Procedure

<u>Set-up (on the day of the titration)</u>:

1. Pierce the cap of the 2.0 mL cryovial containing your protein sample with a needle to allow degassing (see below) without protein foaming. Multiple holes can be made to facilitate faster purging.
2. Place the capped cryovial into a 20 mL scintillation vial and then seal the scintillation vial with a Precision Seal rubber septum.
3. Pierce the septum of the scintillation vial with two Precision Glide needles far apart and then leave the needles in place. One of the needles will be

used as an input for purging with high-purity N_2 gas and the other will serve as the vent during purging.

4. Attach one of the needles to a syringe filter that is hooked up with the nitrogen gas line. The syringe filter is optional.
5. Purge the scintillation vial with nitrogen for 1 to 2 hours while keeping the vial on ice and shielded from light using the aluminum foil.
6. Remove both needles and transfer the scintillation vial into the anaerobic chamber.
7. Store your protein sample in the Ecotherm chilling dry bath at 3 °C, shielded from light, inside the anaerobic chamber.
8. Make all solutions anaerobic by multiple cycles of alternating pumping and refilling with purified N_2 or Ar gas, on a gas train. Similarly, all dry reagents should be weighed out into septum vials, then their head spaces should be made fully anaerobic.
9. Transfer stable reagents into the anaerobic chamber and allow them to equilibrate with the intert atmosphere. Note that some protein samples undergo slow auto-reduction under anaerobic conditions or may be even unstable *vs*. overnight storage at 3 °C. In these cases, the protein samples should be thawed from -80 °C, made anaerobic on the day of the experiment and used right away, for consistent titration data.
10. Shield methyl viologen and reference dyes from light with aluminum foil.
11. Keep xanthine oxidase and any other labile reagents in the Ecotherm chilling dry bath at 3 °C.

To initiate the titration

12. If needed, pretreat the enzyme sample with 0.5 mM ferricyanide, to obtain a starting state of 100% in the oxidized state. Then pass the enzyme over a gel filtration minicolumn to remove oxidant.
13. Place 385 µL of 520 µM xanthine in a 500 µL self-masking cuvette and collect a spectrum to serve as the blank reference.
14. Add 5 µL of 100 µM methyl viologen, mix well with a micro stirring bar and then record another spectrum. There should be no apparent absorbance in the 300-800 nm region, indicating that the methyl viologen is in the oxidized state. (Collect a mediator blank spectrum.)
15. Add 100 µL of your enzyme to produce a concentration of at minimum 10 µM. Mix gently and well, then record the starting oxidized spectrum.
16. Add up to 5 µL of the reference dye and mix gently but thoroughly. Record the spectrum of oxidized protein plus oxidized dye. (The amount of reference dye used in the titration depends on its extinction coefficient. Generally, keep the absorbance of the dye comparable to that of the 450 nm band of the enzyme.)

    The components added are summarized as follows:

Volume (µL)	Component	Final concentration (µM)
385	520 µM xanthine	400
5	100 µM methyl viologen	1
100	≥50 µM enzyme	≥10
5	reference dye	-

17. To initiate the titration, add 5 µL of 1 µM xanthine oxidase (10 nM final concentration). Mix thoroughly and collect a spectrum every 1 min from 200-800 nm (or further if possible). The rate of reduction is controlled by the concentration of xanthine oxidase with a larger amount of enzyme producing more rapid reduction. Therefore, a trial run is usually necessary to find a good concentration of xanthine oxidase which allows the titration to last 1-2 hours. Too rapid a titration can preclude maintenance of equilibrium.

5 Ingredients of Success: Tips

Every enzyme is different so the advice that follows will need to be filtered and optimized for the specific system of interest.

Self-masking quartz cuvettes permit use of as little as 0.5 mL of sample, at flavin concentrations of no less than 10 µM. Even when used in an anaerobic chamber, an airtight screw-cap cuvette is helpful.

In our work, reducing equivalents have been provided continuously by including xanthine and xanthine oxidase in the reaction following the procedure of (Massey, 1991). We use a 0.5 ml reaction containing 400 µM xanthine, 1 µM methyl viologen (mediator), 10 µM *Rpal*ETF and a concentration of the reference dye that yields comparable absorbance to that of the flavins in the buffer of choice (Efimov et al., 2014; Mishanina et al., 2015). The reaction is initiated by adding a catalytic amount of xanthine oxidase (0.5-20 nM) with a larger amount used for titrations aiming for more reduced states of the ETF. Spectral changes are monitored every 1 min. Analyses

exploit spectra demonstrating concurrent reduction of the reference dye and progress of the flavin reduction of interest.

5.1- Identification of the species formed, isosbestic and characteristic wavelengths.

It is helpful to begin the investigation by performing reductive titrations in the absence of dyes, to learn what oxidation states are formed with different reductants and oxidants, and to determine the absorbance maxima and isosbetic wavelengths. Difference spectra characterizing the different stages of the titration will identify the wavelengths at which measurements are maximally sensitive to the oxidation state change for each of the flavin and the dye. It is ideal if a wavelength that is an isosbestic for the flavin can be used to monitor the oxidation state of the dye, and *vice versa*. Alternatively, if a sufficient portion of the dye's signal is non-overlapping with the flavin, then this region can be used both to determine the fraction of dye that is oxidized and to determine the weighting factor needed to subtract the contribution of the dye from the rest of the spectrum, using the previously obtained spectrum of dye alone.

Thus, a titration with dithionite revealed that one of the FADs in Bf-ETF undergoes sequential $1e^-$ reduction via an ASQ state whereas the other undergoes concerted $2e^-$ reduction from OX to HQ, for *R. palustris* ETF (*Rpal*ETF). Titration with NADH as the reductant revealed a qualitatively identical result for *Rpal*ETF, as for the Bf-ETFs from *Acetaminococcus fermentans* and *Megasphaera elsdenii* (Chowdhury et al., 2015; Chowdhury et al., 2014; Sato et al., 2013). However mutant *Rpal*ETF lacking the Bf-FAD was not susceptible to reduction by NADH, whereas Bf-ETF from *Megasphaera elsdenii* containing only the Bf-FAD underwent only $2e^-$ reduction without accumulating any SQ (Sato et al., 2013). Titrations in which proteins serve to deliver reducing or

oxidizing equivalents are also invaluable (Chowdhury et al., 2014). (Note that given the absence of mediator, it can happen that a long-lived kinetic intermediate is formed, which may require that mediators or partner proteins be provided (Talfournier et al., 2001).)

Figure 5A shows the sequence of spectra collected for *Rpal*ETF in the course of a titration using dithionite as the reductant. Resulting spectra show an initial increase at 374 nm indicative of ASQ formation while a decrease at 456 nm reveals diminution of OX. Later in the titration intensity decreases at all wavelengths producing a typical OX spectrum roughly half way through that then gives way to the weak signal of HQ. Plots of the absorbance at the absorption maxima of the different species chart their appearance and disappearance (Figure 5B, (Byron et al., 1989; Duan et al., 2018; Mayhew et al., 1969; Sevrioukova et al., 1996; Swenson and Krey, 1994)). Three phases are readily distinguished (Figure 5B).

Figure 5 here.

5.2- Nature of the reaction in each phase of the titration and calculation of flavin populations, oxidized and reduced.

The nature of the reaction characterizing each phase can be determined by difference spectra calculated for each phase of the titration, as the first spectrum for the phase minus the last one (Figure 6A). Comparison with synthetic difference spectra constructed from spectra that typify each of the flavin oxidation states in well-studied systems confirms that the dominant process in the first phase is conversion of OX to ASQ (Figure 6B), the second phase is best described by conversion of ASQ to HQ and the third phase is OX to HQ. The difference spectra in Figure 6A also reveal which

wavelengths are maximally sensitive to the change being monitored, which may not be the same as the wavelengths with the maximum absorbance (Figure 7A). Division of the ΔA at the chose wavelength by the concentration change yields a difference extinction coefficient.

Figure 6 here.

It is equally easy to note that the full difference for the phase represents a population change of 1. Then, subtraction of the last spectrum of a phase from all preceding spectra yields the same difference but with a decreasing amplitude representing the extent to which the population is approaching the final state. The amplitude of difference spectrum 'i' divided by that of the complete phase ($\Delta_{(phase)}$) yields the population change it represents. Addition of the change to the starting population mix yields [Ox] and [Red] (Scheme 1).

Scheme 1 here.

5.3- Calculation of oxidized and reduced populations of indicator dye

The spectra obtained in the course of an E° measurement are more complicated because they include the indicator dye in addition to the flavin. The dyes are chosen to provide a reference E° near that of the flavin (usually within 30 mV) but also to not interfere with the flavin's optical signals. Figure 7 shows spectra of three of our favorites in panel B, compared with the signatures of different flavin oxidation states in panel A. A concentration of indicator dye yielding an optical amplitude comparable to that of the flavin is usually chosen. While it may not be possible to find a dye that does not overlap with the flavin signals, the dye's oxidized-state amplitude can nonetheless be determined at a wavelength that is an isosbestic for the flavin oxidation state under

study. Thus, at the wavelength at which the flavin OX and ASQ spectra cross, any change in absorbance will be attributable to the dye's change in oxidation state as the titration proceeds. Knowledge of the progress of the dye's reduction then permits subtraction of the dye's contribution to the optical spectrum, for each step in the phase, and analysis for flavin populations as above. Alternately, a set of simultaneous equations can be used to account for conversion to the reduced states of flavin and dye in each reduction phase (Trimmer et al., 2005).

Figure 7 here.

5.4- Log/Log plots of population ratios.

For the example of OX → ASQ (Phase 1) 4.2 μM methylene blue was included and its oxidized population monitored at 664 nm using the extinction coefficient ε_{664} = 76 mM^{-1} cm^{-1}, $E°'$= +11 mV (Norden and Tjerneld, 1982) while the population of ET-FAD converted to ASQ was determined from difference spectra and $\Delta\varepsilon_{456}(ET\text{-}FAD_{OX\text{-}SQ})$ = 6.57 mM^{-1} cm^{-1} (Duan et al., 2018). Panel A shows the difference spectra obtained for this phase as per scheme 1, Panel B shows the result of deconvolution of the spectrum of methylene blue, accounting for its increasing extent of reduction. At the wavelength used to evaluate the extent of flavin reduction, the contribution of this dye is very small, and moreover corrected out.

Figure 8 here.

Using the determined populations of Ox and Red flavin and dye, a plot of $\ln([FAD_{Ox}]/[FAD_{Red}])$ vs. $\ln([Dye_{Ox}]/[Dye_{Red}])$ is fit with a linear regression model corresponding to Equation 8 (see equation 5).

$$ln\left(\frac{[\mathrm{F_{Ox}}]}{[\mathrm{F_{Red}}]}\right) = b + \frac{\mathrm{n_F}}{\mathrm{n_D}}\, ln\left(\frac{[\mathrm{D_{Ox}}]}{[\mathrm{D_{Red}}]}\right) \qquad (8A)$$

where *b* is the intercept produced by the fit. For methylene blue, $n_D = 2$. Thus the obtained slope of 0.51 confirms the spectral signatures in assigning the reaction to $1e^-$ reduction of OX to ASQ.

The value obtained for *b* was then used with the midpoint potential of the dye at the pH used to calculate the *E*°.

$$b = \frac{n_F}{25.7\ mV}(E_D^0 - E_F^0) \qquad (8B)$$

where 25.7 mV replaces *RT/F*. In this case, because the measurement was made at pH 9, we calculated the dye $E°_D$ at that pH to be -48 mV from the published *E°′* value of 11 mV and a correction of -59mV/2 per pH unit increase consistent with acquisition of one proton per two electrons in the range of pH 7 - 9 for methylene blue (Norden and Tjerneld, 1982). Thus for the example of the intercept in Figure 8C we have that -0.13 = (-48 mV - E_F^0)/25.7 mV so -45 mV = E_F^0. Since the OX/ASQ reduction does not involve any protons, the value of *E*° is pH independent. Three independent repetitions yielded an average $E°_{OX/ASQ}$ of -47 ± 4 mV for this system (Duan et al., 2018).

6 Controls and precautions

6.1- Enzyme Integrity

It is crucial that the enzyme retain its integrity throughout collection of the data set, so that all the data can be considered to represent the same condition of the enzyme, albeit at different ratios of oxidation states. The most important consideration is that no cofactors should be released, as free flavin (or other cofactor) will contribute to the spectra but introduce additional species that will be essentially impossible to deconvolute from the species of interest. At the end of a titration, it is good practice to assay enzyme activity when an assay exists, for comparison with activity beforehand.

Passage of the sample over a gel filtration column (in the anaerobic chamber) is recommended to separate the enzyme from all mediators, dyes and titrants to permit assessment of any flavin release via an optical spectrum of the small-molecule fraction after reoxidation. Similarly, the recovered enzyme upon reoxidation should display the same optical spectrum as it did beforehand.

If the enzyme does not tolerate a full titration (typically taking 1-2 hours, but in some cases requiring days (Byron et al., 1989)), then it is better to make a series of short measurements by setting up several individual equilibrations with different amounts of reductant (oxidant) and monitoring each for approach to equilibrium. Single exponential kinetics are anticipated and the equilibrium point can often be predicted with good accuracy without waiting for it to be achieved (an asymptotic process that becomes increasingly slow) (Anderson, 1983).

Figure 9 here.

6.2- Non-Interference by Dyes

Mediators and dyes that are intended to accelerate equilibration of the electrode with the rest of the system need to populate their SQ states or at least have thermal access to them in order to be effective (Dutton, 1978). They should ideally also have $E°$s within 30 mV of the target value of the experiment. However if they are additionally to serve as the means of measuring E, they must be present at a concentration sufficient that spectral changes corresponding to ≈ 2 mV can be measured reproducibly. Since spectra of the flavin are also desired (unless EPR will be used to measure flavin SQ concentrations), the best dyes have optical spectra that minimally overlap with the signatures of the flavin. This must be true for both oxidation states of the dye. A dye that

interacts preferentially with one or other oxidation state of the enzyme can shift the enzyme's apparent *E*° via the binding equilibrium. In cases where a different dye cannot be found, measurements at a series of dye concentrations permit extraction of the enzyme *E*° corresponding to no binding of dye (for example (Koder and Miller, 1998)). As a compromise between provision of enough dye to permit rapid equilibration, but not so much as to obscure the optical signals of the flavin, many authors employ a concentration that produces a similar maximum absorbance to that of the flavin (Mishanina et al., 2015), or comparable concentration (Pitsawong et al., 2010).

Obviously the dyes should be pure. In many cases this will require that they be recrystallized prior to use, as some are photochemically labile and a bottle may be decades old and still in use. Storage in the dark with an Ar head space or in Ar-filled secondary containment is recommended for some. Since some of the mediator/dyes are toxic and carcinogenic, self-education and due precautions are essential. The optical spectrum of the dye should not be altered by addition of the enzyme, as this could indicate reaction between the two, and the dyes should not succumb to reaction in the course of the titration, as confirmed by the optical spectrum of the small molecules separated from the enzyme, after the titration (above). The titration should be protected from light to minimize photochemically driven reactions of photosensitive dyes as well as the flavin.

6.3- Anaerobicity

Prepare all solutions, apparatus and reagents to be fully anaerobic before beginning the titration, and keep everything that way. We degas large volumes on a gas train and then move them into an anaerobic chamber the night before use. To do

this, bubble scrubbed Ar through large volumes of buffer while stirring. Recall that the solubility of O_2 is higher in cold aqueous solutions than in warm ones so allow refrigerated solutions to come to room temperature before degassing. For small volumes, 5 cycles of evacuation and refilling with scrubbed Ar while stirring is generally sufficient. Sets of pipettors and syringes reside permanently in the chamber. Protein samples are brought into the chamber on the day of use and are kept in a chilling dry bath shielded from light, along with stock solutions of the mediators and short-lived reactants such as NADH or dithionite. The chilling dry bath is very helpful.

We also have the luxury of a spectrophotometer inside the anaerobic chamber, this has made a big difference to the quality of our results and greatly diminishes the stress involved in performance of the experiments. A few other metrics for success are provided in graphical format, please see Figure 10.

Figure 10 here.

6.4- Chemical Titrants

Sodium dithionite is able to produce *E* values as low as -420 mV and is essentially colorless (Dutton, 1978), but tends to be impure as purchased and has a signal at 315 nm which is a useful indication at the end of a reductive titration that the sample is no longer reacting with added reductant. However the products of dithionite oxidation are acidic so the stock solution should be well buffered. In addition, dithionite solutions have a limited shelf life. We prefer to make them up in degassed buffer immediately before use, keep them cold under inert atmosphere and use them within 6 hours. A solution buffered at high pH (e.g., 12) will last longer. Best practice is to test the solution regularly by depositing a drop onto a piece of filter paper that has been wet with methyl

viologen and allowed to dry. A solution retaining reducing activity will create a purple spot which will fade quickly in air, but persist in a good inert atmosphere. Methyl viologen is toxic and must be handled with due precaution, but it is helpful to prepare a small stash of filter papers dipped in methyl violagen, dried and then cut into 1 cm squares. These can be stored conveniently in small stoppered vials for use at gas trains or in glove boxes. They should be handled with tweezers or gloves and disposed of as toxic, but provide immediate diagnosis of solutions.

Ferricyanide can produce a solution *E* up to +400 mV, using only a few µL of 100 mM stock solution. This suffices to produce a spectrum of fully oxidized enzyme.

As with any other measurement, results should be repeatable for different preparations of the enzyme. Ideally it should be possible to confirm reversibility and independence from the rate at which the titration is performed (confirms absence of a kinetic limit). The value of $E°$ should not depend on the identity of the mediator/dye.

At the end of a reductive titration, it is valuable to confirm the end-point via full reduction using dithionite, and for oxidative titrations ferricyanide can be used (but obtain spectra of ferri and ferrocyanide as the former contributes a yellow color of its own (Dutton, 1978)).

7 Concluding Remarks

Careful study of metabolic energetics was crucial in revealing the importance of bifurcation to life (Buckel and Thauer, 2013; Nitschke and Russell, 2012). Similarly, determination of the $E°$s of individual sites contributing to this activity can educate us as to the mechanisms used to execute bifurcation in enzymes. Since these provide means of optimizing energy conservation and versatility, we hope that increased understanding

of enzymatic bifurcation can inspire more efficient man-made materials and devices, allowing us to lighten the load we place on our planet's ecosystems.

References

Alric, J., Pierre, Y., Picot, D., Lavergne, J., and Rappaport, F. (2005). Spectral and redox characterization of the heme ci of the cytochrome b6f complex. Proc Natl Acad Sci U S A *102*, 15860-15865.

Anderson, R.F. (1983). Energetics of the one-electron reduction steps of riboflavin, FMN and FAD to their fully reduced forms. Biochim Biophys Acta *722*, 158-162.

Arents, J.C., Perez, M.A., Hendriks, J., and Hellingwerf, K.J. (2011). On the midpoint potential of the FAD chromophore in a BLUF-domain containing photoreceptor protein. FEBS Lett *585*, 167-172.

Brugna, M., Albouy, D., and Nitschke, W. (1998). Diversity of cytochrome bc complexes: example of the Rieske protein in green sulfur bacteria. Journal of bacteriology *180*, 3719-3723.

Buckel, W., and Thauer, R.K. (2013). Energy conservation via electron bifurcating ferredoxin reduction and proton/Na+ translocating ferredoxin oxidation. Biochim Biophys Acta *1827*, 94-113.

Buckel, W., and Thauer, R.K. (2018). Flavin-based electron bifurcation, a new mechanism of biological energy coupling. Chem Rev *118*.

Byron, C.M., Stankovich, M.T., Husain, M., and Davidson, V.L. (1989). Unusual Redox Properties of Electron-Transfer Flavoprotein from *Methylophilus methylotrophus*. Biochemistry *28*, 8582-8587.

Chen, L., Liu, M.Y., Legall, J., Fareleira, P., Santos, H., and Xavier, A.V. (1993). Purification and characterization of an NADH-rubredoxin oxidoreductase involved in the utilization of oxygen by Desulfovibrio gigas. Eur J Biochem *216*, 443-448.

Cheng, V.W., Tran, Q.M., Boroumand, N., Rothery, R.A., Maklashina, E., Cecchini, G., and Weiner, J.H. (2013). A conserved lysine residue controls iron-sulfur cluster redox chemistry in Escherichia coli fumarate reductase. Biochim Biophys Acta *1827*, 1141-1147.

Chowdhury, N.P., Kahnt, J., and Buckel, W. (2015). Reduction of ferredoxin or oxygen by flavin-based electron bifurcation in Megasphaera elsdenii. FEBS J *282*, 3149-3160.

Chowdhury, N.P., Mowafy, A.M., Demmer, J.K., Upadhyay, V., Koelzer, S., Jayamani, E., Kahnt, J., Hornung, M., Demmer, U., Ermler, U*., et al.* (2014). Studies on the Mechanism of Electron Bifurcation Catalyzed by Electron Transferring Flavoprotein (Etf) and Butyryl-CoA Dehydrogenase (Bcd) of *Acidaminococcus fermentans*. J Biol Chem *289*, 5145-5157.

Clark, W.M. (1960). Oxidation-Reduction Potentials of Organic Systems (Baltimore MD: Williams and Wilkins).

Corrado, M.E., Aliverti, A., Zanetti, G., and Mayhew, S.G. (1996). Analysis of the oxidation-reduction potentials of recombinant ferredoxin-NADP+ reductase from spinach chloroplasts. Eur J Biochem *239*, 662-667.

Covian, R., Zwicker, K., Rotsaert, F.A., and Trumpower, B.L. (2007). Asymmetric and redox-specific binding of quinone and quinol at center N of the dimeric yeast

cytochrome bc1 complex. Consequences for semiquinone stabilization. J Biol Chem *282*, 24198-24208.
Demmer, J.K., Chowdhury, N.P., Selmer, T., Ermler, U., and Buckel, W. (2017). The semiquinone swing in the bifurcating electron transferring flavoprotein/butyryl-coA dehydrogenase complex from Clostridium difficile. Nat Commun *8*.
Demmer, J.K., Huang, H., Wang, S., Demmer, U., Thauer, R.K., and Ermler, U. (2015). Insights into flavin-based electron bifurcation via the NADH-dependent reduced ferredoxin:NADP oxidoreductase structure. J Biol Chem *290*, 21985-21995.
Duan, H.D., Lubner, C.E., Tokmina-Lukaszewska, M., Gauss, G.H., Bothner, B., King, P.W., Peters, J.W., and Miller, A.F. (2018). Distinct flavin properties underlie flavin-based electron bifurcation within a novel electron-transferring flavoprotein FixAB from *Rhodopseudomonas palustris*. J Biol Chem *293*, 4688-4701.
Dutton, P.L. (1978). Redox potentiometry: Determination of midpoint potentials of oxidation-reduction components of biological electron-transfer systems. Meth Enzymol *54*, 411-435.
Efimov, I., Parkin, G., Millett, E.S., Glenday, J., Chan, C.K., Weedon, H., Randhawa, H., Basran, J., and Raven, E.L. (2014). A simple method for the determination of reduction potentials in heme proteins. FEBS Lett *588*, 701-704.
Ehrenberg, A., Müller, F., and Hemmerich, P. (1967). Basicity, visible spectra an delectron spin resonance of flavosemiquinone anions. Eur J Biochem *2*, 282-293.
Garcia Costas, A.M., Poudel, S., Miller, A.-F., J., S.G., Ledbetter, R.N., Fixen, K., Seefeldt, L.C., Adams, M.W., Harwood, C.S., Boyd, E.S.*, et al.* (2017). Defining Electron Bifurcation in the Electron Transferring Flavoprotein Family. J Bacteriol.
Guerrero, F., Sedoud, A., Kirilovsky, D., Rutherford, A.W., Ortega, J.M., and Roncel, M. (2011). A high redox potential form of cytochrome c550 in photosystem II from Thermosynechococcus elongatus. J Biol Chem *286*, 5985-5994.
Haid, E., Lehmann, P., and Ziegenhorn, J. (1975). Molar absorptivities of beta-NADH and beta-NAD at 260 nm. Clinical chemistry *21*, 884-887.
Herrmann, G., Jayamani, E., Mai, G., and Buckel, W. (2008). Energy conservation via electron-transferring flavoprotein in anaerobic bacteria. J Bacteriol *190*, 784-791.
Hirst, J. (2010). Towards the molecular mechanism of respiratory complex I. Biochem J *425*, 327-339.
Hoben, J.P., Lubner, C.E., Ratzloff, M.W., Schut, G.J., Nguyen, D.M.N., Hempel, K.W., Adams, M.W.W., King, P.W., and Miller, A.F. (2017). Equilibrium and ultrafast kinetic studies manipulating electron transfer: A short-lived flavin semiquinone is not sufficient for electron bifurcation. J Biol Chem *292*, 14039-14049.
Hu, J., Chuenchor, W., and Rokita, S.E. (2015). A switch between one- and two-electron chemistry of the human flavoprotein iodotyrosine deiodinase is controlled by substrate. The Journal of biological chemistry *290*, 590-600.
Jang, M.H., Scrutton, N.S., and Hille, R. (2000). Formation of W(3)A(1) electron-transferring flavoprotein (ETF) hydroquinone in the trimethylamine dehydrogenase x ETF protein complex. The Journal of biological chemistry *275*, 12546-12552.
Jung, Y.S., Vassiliev, I.R., Qiao, F., Yang, F., Bryant, D.A., and Golbeck, J.H. (1996). Modified ligands to FA and FB in photosystem I. Proposed chemical rescue of a [4Fe-4S] cluster with an external thiolate in alanine, glycine, and serine mutants of PsaC. J Biol Chem *271*, 31135-31144.

Kay, C.J., Solomonson, L.P., and Barber, M.J. (1986). Thermodynamic properties of the heme prosthetic group in assimilatory nitrate reductase. J Biol Chem *261*, 5799-5802.
Koder, R.L., Haynes, C.A., Rodgers, M.E., Rodgers, D.W., and Miller, A.-F. (2002). Flavin thermodynamics explain the oxygen insensitivity of enteric nitroreductases. Biochemistry *41*, 14197-14205.
Koder, R.L., Jr., and Miller, A.-F. (1998). Steady state kinetic mechanism, stereospecificity, substrate and inhibitor specificity of Enterobacter cloacae nitroreductase. Biochim Biophys Acta *1387*, 394-405.
Kolaj-Robin, O., O'Kane, S.R., Nitschke, W., Leger, C., Baymann, F., and Soulimane, T. (2011). Biochemical and biophysical characterization of succinate: quinone reductase from Thermus thermophilus. Biochim Biophys Acta *1807*, 68-79.
Ledbetter, R.N., Garcia Costas, A.M., Lubner, C.E., Mulder, D.E., Tokmina-Lukaszewska, M., Artz, J.H., Patterson, A., Magnuson, T.S., Jay, Z.J., Duan, H.D.*, et al.* (2017). The Electron Bifurcating FixABCX Protein Complex from Azotobacter vinelandii: Generation of Low-Potential Reducing Equivalents for Nitrogenase Catalysis. Biochemistry *56*, 4177-4190.
Lubner, C.E., Jennings, D.P., Mulder, D.W., Schut, G.J., Zadvornyy, O.A., Hoben, J.P., Tokmina-Lukaszewska, M., Berry, L., Nguyen, D.M., Lipscomb, G.L.*, et al.* (2017). Mechanistic insights into energy conservation by flavin-based electron bifurcation. Nat Chem Biol *13*, 655-659.
Massey, V. (1991). A simple method for determination of redox potentials. In Flavins and flavoproteins, B. Curti, S. Ronchi, and G. Zanetti, eds. (Berlin: Walter de Gruyer), pp. 59-66.
Matsui, T., Kitagawa, Y., Okumura, M., and Shigeta, Y. (2015). Accurate standard hydrogen electrode potential and applications to the redox potentials of vitamin C and NAD/NADH. J Phys Chem A *119*, 369-376.
Mayhew, S.G. (1978). The redox potential of dithionite and SO_2^- from equilibrium reactions with flavodoxins, methyl viologen and hydrogen plus hydrogenase. Eur J Biochem *85*.
Mayhew, S.G. (1999a). The Effects of pH and Semiquinone Formation on the Oxidation-Reduction Potentials of Flavin Mononucleotide: A Reappraisal. Eur J Biochem *265*, 698-702.
Mayhew, S.G. (1999b). Potentiometric measurements of oxidation-reduction potentials. In Flavoprotein Protocols, S.K. Chapman, and G.A. Reid, eds. (Totowa, NJ: Humana Press), pp. 49-59.
Mayhew, S.G., Foust, G.P., and Massey, V. (1969). Oxidation-reduction properties of flavodoxin from *Peptostreptococcus elsdenii*. J Biol Chem *244*, 803-810.
Millner, P.A., Widger, W.R., Abbott, M.S., Cramer, W.A., and Dilley, R.A. (1982). The effect of adenine nucleotides on inhibition of the thylakoid protein kinase by sulfhydryl-directed reagents. J Biol Chem *257*, 1736-1742.
Mishanina, T.V., Yadav, P.K., Ballou, D.P., and Banerjee, R. (2015). Transient Kinetic Analysis of Hydrogen Sulfide Oxidation Catalyzed by Human Sulfide Quinone Oxidoreductase. J Biol Chem *290*, 25072-25080.

Nakajima, H., Honma, Y., Tawara, T., Kato, T., Park, S.Y., Miyatake, H., Shiro, Y., and Aono, S. (2001). Redox properties and coordination structure of the heme in the co-sensing transcriptional activator CooA. J Biol Chem *276*, 7055-7061.
Nedbal, L., Samson, G., and Whitmarsh, J. (1992). Redox state of a one-electron component controls the rate of photoinhibition of photosystem II. Proc Natl Acad Sci U S A *89*, 7929-7933.
Nitschke, W., and Russell, M.J. (2012). Redox bifurcations: Mechanisms and importance to life now, and at its origin. Bioessays *34*, 106-109.
Norden, B., and Tjerneld, F. (1982). Structure of methylene blue-DNA complexes studied by linear and circular dichroism spectroscopy. Biopolymers *21*, 1713-1734.
O'Farrel, P.A., Walsh, M.A., McCarthy, A.A., Higgins, T.M., Voordouw, G., and Mayhew, S.G. (1998). Modulation of the redox potentials of FMN in Desulfovibrio vulgaris flavodoxin: thermodynamic properties and crystal structures of glycine-61 mutants. Biochemistry *37*, 8405-8416.
Ottaway, J.M. (1972). Oxidation-reduction indicators of E'2 < 0.76 Volt. In Indicators, E. Bishop, ed. (New York: Pergamon), pp. 469-528.
Pitsawong, W., Jeerus, S., Methinee, P., Tan, T.-C., Spadiut, O., Haltrich, D., Divne, C., and Chaiyen, P. (2010). A Conserved Active-site Threonine Is Important for Both Sugar and Flavin Oxidations of Pyranose 2-Oxidase. J Biol Chem *285*, 9697-9705.
Pueyo, J.J., Gomez-Moreno, C., and Mayhew, S.G. (1991). Oxidation-reduction potentials of ferredoxin-NADP+ reductase and flavodoxin from Anabaena PCC 7119 and their electrostatic and covalent complexes. Eur J Biochem *202*, 1065-1071.
Sato, K., Nishina, Y., and Shiga, K. (1993). Electron-transferring flavoprotein has an AMP-binding site in addition to the FAD-binding site. J Biochem *114*, 215-222.
Sato, K., Nishina, Y., and Shiga, K. (2003). Purification of electron-transferring flavoprotein from Megasphaera elsdenii and binding of additional FAD with an unusual absorption spectrum. J Biochem *134*, 719-729.
Sato, K., Nishina, Y., and Shiga, K. (2013). Interaction between NADH and electron-transferring flavoprotein from *Megasphaera elsdenii*. J Biochem *153*, 565-572.
Sevrioukova, I., Shaffer, C., Ballou, D.P., and Peterson, J.A. (1996). Equilibrium and transient state spectrophotometric studies of the mechanism of reduction of the flavoprotein domain of P450BM-3. Biochem *35*, 7058-7068.
Stankovich, M.T., Schopfer, L.M., and Massey, V. (1978). Determination of glucose oxidase oxidation-reduction potentials and the oxygen reactivity of fully reduced and semiquinoid forms. J Biol Chem *253*, 4971-4979.
Swenson, R.P., and Krey, G.D. (1994). Site-directed mutagenesis of Tyrosine-98 in the flavodoxin from *Desulfovibrio vulgaris* (Hildenborough): Regulation of the oxidation-reduction properties of the bound FMN cofactor by aromatic, solvent and electrostatic interactions. Biochemistry *33*, 8505-8514.
Talfournier, F., Munro, A.W., Basran, J., Sutcliffe, M.J., Daff, S., Chapman, S.K., and Scrutton, N.S. (2001). alpha Arg-237 in Methylophilus methylotrophus (sp. W3A1) electron-transferring flavoprotein affords approximately 200-millivolt stabilization of the FAD anionic semiquinone and a kinetic block on full reduction to the dihydroquinone. J Biol Chem *276*, 20190-20196.

Trimmer, E.E., Ballou, D.P., Galloway, L.J., Scannell, S.A., Brinker, D.R., and Casas, K.R. (2005). Aspartate 120 of Escherichia coli Methylenetetrahydrofolate Reductase: Evidence for Major Roles in Folate Binding and Catalysis and a Minor Role in Flavin Reactivity. Biochem *44*, 6809-6822.

Tyree, B., and Webster, D.A. (1978). Electron-accepting properties of cytochrome o purified from Vitreoscilla. J Biol Chem *253*, 7635-7637.

Ugulava, N.B., and Crofts, A.R. (1998). CD-monitored redox titration of the Rieske Fe-S protein of Rhodobacter sphaeroides: pH dependence of the midpoint potential in isolated bc1 complex and in membranes. FEBS Lett *440*, 409-413.

Vollmer, S.J., Switzer, R.L., and Debrunner, P.G. (1983). Oxidation-reduction properties of the iron-sulfur cluster in Bacillus subtilis glutamine phosphoribosylpyrophosphate amidotransferase. J Biol Chem *258*, 14284-14293.

Watmough, N.J., and Frerman, F.E. (2010). The electron transfer flavoprotein: Ubiquinone oxidoreductases. Biochim Biophys Acta *1797*, 1910-1916.

Winkler, A., Motz, K., Riedl, S., Puhl, M., Macheroux, P., and Gruber, K. (2009). Structural and mechanistic studies reveal the functional role of bicovalent flavinylation in berberine bridge enzyme. J Biol Chem *284*, 19993-20001.

Zhang, H., Carrell, C.J., Huang, D., Sled, V., Ohnishi, T., Smith, J.L., and Cramer, W.A. (1996). Characterization and crystallization of the lumen side domain of the chloroplast Rieske iron-sulfur protein. J Biol Chem *271*, 31360-31366.

Zhang, P., Yuly, J.L., Lubner, C.E., Mulder, D.W., King, P.W., Peters, J.W., and Beratan, D.N. (2017). Electron Bifurcation: Thermodynamics and Kinetics of Two-Electron Brokering in Biological Redox Chemistry. Acc Chem Res *50*, 2410-2417.

Zhu, J., Egawa, T., Yeh, S.R., Yu, L., and Yu, C.A. (2007). Simultaneous reduction of iron-sulfur protein and cytochrome b(L) during ubiquinol oxidation in cytochrome bc(1) complex. Proc Natl Acad Sci U S A *104*, 4864-4869.

Zhu, Z., and Davidson, V.L. (1998). Redox properties of tryptophan tryptophylquinone enzymes. Correlation with structure and reactivity. J Biol Chem *273*, 14254-14260.

Table 1. Some useful reference dyes and mediators[a]

Name	$E°$ / mV (vs. NHE)	Number of electrons/n
Potassium Ferricyanide (Guerrero et al., 2011)	430	1
p-benzoquinone (Guerrero et al., 2011)	280	2
N,N,N',N',-tetramethyl phenylene diamine (Zhang et al., 1996)	260	1
Diaminodurol (Guerrero et al., 2011)	220	2
2,6-dichlorophenolindophenol (Kolaj-Robin et al., 201	217	2
2,5-dimethyl benzoquinone (Brugna et al., 1998)	180	2
Toluylene blue (Tyree and Webster, 1978)	115	2
Phenazine methosulfate (Zhu and Davidson, 1998)	80	2
Thionine (Jung et al., 1996)	56	2
Phenazine ethosulfate (Covian et al., 2007)	55	2
Toluidine blue (Winkler et al., 2009)	34	2
Ascorbate (Matsui et al., 2015)	30	2
Gallocyanine (Nakajima et al., 2001)	21	2
Methylene blue (Vollmer et al., 1983)	11	2
Duroquinone (Nedbal et al., 1992)	5	2
Menadione (Alric et al., 2005)	0	2
Pyocyanine (Ugulava and Crofts, 1998)	-34	2
5,5',7,7'-indigotetrasulphonate (Chen et al., 1993)	-46	2
5,5',7-indigotrisulphonate (Chen et al., 1993)	-81	2

5,5’-indigodisulphonate (Cheng et al., 2013)	-125	2
Nile Blue (Hu et al., 2015)	-116	2
2-hydroxyl-1,4-naphthoquinone (Kay et al., 1986)	-145	2
Anthraquinone-2,6-disulphonate (Millner et al., 1982)	-185	2
Anthraquinone-2-sulfonate (Guerrero et al., 2011)	-225	2
Phenosafranine (Arents et al., 2011)	-252	2
Safranine T (Arents et al., 2011)	-289	2
Neutral red (Pueyo et al., 1991)	-325 -323	2
Benzyl viologen (Stankovich et al., 1978)	-311	1
Diquat (Chen et al., 1993)	-361	1
Dithionite[b] (Jang et al., 2000)	-386	1
Methyl viologen (Corrado et al., 1996)	-430	1

[a] also see (Clark, 1960; Ottaway, 1972)

[b] Note: dithionite reduction midpoint pontential depends strongly on pH and concentration.

Scheme Legend

Scheme 1. Recipies for calculating populations from difference spectrum amplitudes, for two scenarios. Top: the case where the high-*E*° flavin is fully oxidized at the outset or, below: the case where the high-*E*° flavin is partially reduced at the start, as a consequence of its high E°.

Figure Legends

Figure 1. cartoon of minimal flavin-based bifurcating system, in which the flavin is represented by the green cartoon, a higher-E° cofactor able to accept one electron in an exergonic transfer is in yellow, whereas a lower-E° acceptor whose reduction by the flavin represents an endergonic, energy conserving step, is in orange.

Figure 2. Cartoon of Bf-ETF associated with nitrogen fixation, and its partner proteins the ETF/quinone oxidoreductase (FixC) and the FixX component believed to mediate electron transfer to Fd or Fld.

Figure 3. Dependence on ambient potential of the concentrations of Reduced and Oxidized states for reactions of Ox + $1e^-$ → Red (n=1, dashed lines) and Ox + $2e^-$ → Red (n=2, solid lines). Panel A provides the response of one or other state as a fraction of the total, since it is often the case that only one of the two states is detected directly. Panel B provides the response of the ratio of populations or concentrations after taking

the $\log_{10}$, which provides the benefit of a linear plot in which the slope provides a test of the nature of the reaction via the value of n. Slope of log([Ox]/[Red]) vs. E-E° is *nF/2.303RT*.

Figure 4. generic pH dependence expected for flavins that undergo reduction from OX to ASQ (eg. ET-FAD of Bf-ETF, red), and then reduction to anionic HQ (AHQ, orange), flavins such as that of Fld that undergo $1e^- + 1H^+$ reduction to NSQ (blue) and then $1e^-$ reduction to AHQ or $1e^- + 1H^+$ reduction to neutral HQ (purple), contrasted with expectations for a Bf-flavin undergoing $2e^- + 1H^+$ reduction to AHQ (green, where the active site is assumed to depress the pK for protonation of anionic HQ). Applicable values for $E°_{lim\ low\ pH}$ and pKs are inspired by literature when possible, but otherwise provided as plausible guesses for illustrative purposes. They are 7 for the pK of HQ/AHQ, 11 for the pK of Fld NSQ/ASQ and 5 for the pK of ET-FAD NSQ/ASQ.

Figure 5. A: Absorption spectra of *Rpal*ETF documenting the sequence of species present as the enzyme is reduced by substoichiometric dithionite additions, reproduced from (Duan et al., 2018). A dithionite stock solution producing 15 μM increases in concentration with each addition was used. (The concentration of the dithionite stock solution can be estimated via its absorbance at 315 nm, ε_{315} = 7.05 mM^{-1} cm^{-1} (Mayhew, 1978)). If NADH is the titrant, the concentration of the stock solution can be assessed via ε_{340} = 6.22 mM^{-1} cm^{-1} (Haid et al., 1975)). The *Rpal*ETF concentration was 60 μM. B: Plots of extinction coefficient change at select wavelengths, showing distinct behaviors in different phases of the reduction, and wavelengths at which different trends are

detected. A series of difference spectra were calculated from those in panel A by subtracting the final spectrum of the series from every other spectrum. In the resulting difference spectra, the extinction coefficients at different wavelengths were plotted vs. equivalents of dithionite added as a way of monitoring the formation and decay of different species (B). C: difference spectra derived from the first two phases from whence the last spectrum of phase 2 has been subtracted but a HQ signature derived from the last spectrum has been restored, to depict spectra from the higher-*E*° flavin without interference from the lower-*E*° flavin. This research was originally published in the Journal of Biological Chemistry. Duan, H.D., Lubner, C.E., Tokmina-Lukaszewska, M., Gauss, G.H., Bothner, B., King, P.W., Peters, J.W., and Miller, A.F. "Distinct flavin properties underlie flavin-based electron bifurcation within a novel electron-transferring flavoprotein FixAB from *Rhodopseudomonas palustris*." J. Biol. Chem. 2018; 293:4688-4701. © the American Society for Biochemistry and Molecular Biology *or* © the Author(s) (Duan et al., 2018).

Figure 6. Difference spectra corresponding to each phase of reduction of *Rpal*ETF by dithionite (A), compared to synthetic 'model' spectra (B) produced from spectra of OX, ASQ and HQ obtained from systems in which these states can be fully populated: FAD (pH=7.0), glucose oxidase (pH=10) and FAD (pH=7.0), respectively. This research was originally published in the Journal of Biological Chemistry. Duan, H.D., Lubner, C.E., Tokmina-Lukaszewska, M., Gauss, G.H., Bothner, B., King, P.W., Peters, J.W., and Miller, A.F. "Distinct flavin properties underlie flavin-based electron bifurcation within a novel electron-transferring flavoprotein FixAB from *Rhodopseudomonas*

palustris." J. Biol. Chem. 2018; 293:4688-4701. © the American Society for Biochemistry and Molecular Biology *or* © the Author(s) (Duan et al., 2018).

Figure 7. Optical signatures of each of the common oxidation states of flavin (A) compared with the oxidized-state (OX) and reduced-state (Red) spectra of four commonly-used indicator dyes (B). Flavin OX, ASQ, NSQ and HQ spectra were obtained from systems in which these states can be fully populated: FAD (pH=7.0), glucose oxidase (pH=10), flavodoxin from *Desulfovibrio vulgaris* (pH=7.5) and FAD (pH=7.0), respectively. This research was originally published in the Journal of Biological Chemistry. Hoben, J.P., Lubner, C.E., Ratzloff, M.W., Schut, G.J., Nguyen, D.M.N., Hempel, K.W., Adams, M.W.W., King, P.W., and Miller, A.F. "Equilibrium and ultrafast kinetic studies manipulating electron transfer: A short-lived flavin semiquinone is not sufficient for electron bifurcation." J. Biol. Chem. 2017; *292*:14039-14049. © the American Society for Biochemistry and Molecular Biology *or* © the Author(s). (Hoben et al., 2017).

Figure 8. Difference spectra from Phase 1 of reduction of 50 μM *Rpal*ETF in the presence of 4.2 μM of the indicator dye methylene blue. In panel A, the short blue arrow indicates λ_{max} for the dye, used to determine the oxidized population, and the black arrow marks the position at which the difference in *Rpal*ETF population was measured, to be converted to populations OX and ASQ after correction for contribution of the dye (pabel B) as in Scheme 1. Panel C shows the resuling 'log/log' plot where the natural logarithms of the population ratios are plotted for flavin Ox = OX and Red = ASQ, and

dye = methylene blue (MB). This research was originally published in the Journal of Biological Chemistry. Duan, H.D., Lubner, C.E., Tokmina-Lukaszewska, M., Gauss, G.H., Bothner, B., King, P.W., Peters, J.W., and Miller, A.F. "Distinct flavin properties underlie flavin-based electron bifurcation within a novel electron-transferring flavoprotein FixAB from *Rhodopseudomonas palustris*." J. Biol. Chem. 2018; 293:4688-4701. © the American Society for Biochemistry and Molecular Biology *or* © the Author(s) (Duan et al., 2018).

Figure 9. A text-book titration of flavodoxin with dithionite as the reductant, showing desirable features such as clean isosbestics for each successive reaction (black arrows), as well as the increase at 315 nm at the end (pink arrow) indicating that the Fld is fully reduced and excess dithionite is no longer reacting, but accumulating instead. In panel A, OX Fld (heavy red trace) is converted to NSQ (black trace). In panel B Fld NSQ (heavy red trace) is converted to HQ (black trace). *D. vulgaris* Fld was at pH 7.5, and divets due to spectrophotometer problems are evident at 486, 582 and 656 nm.

Figure 10. Cartoon guide to obtaining excellent data, in geek game format.

Schemes

Calculation of populations from difference spectra

Spectra	Diff. spectra = Current - End	=
Start = 1.0 Ox + 0.0 Red	Δ Start=1.0 Ox - 1.0 Red	1.0 $\Delta_{(Phase)}$
Step 1 = 0.8 Ox +0.2 Red	Δ 1 = 0.8 Ox -0.8 Red	0.8 $\Delta_{(Phase)}$
Step 2 = 0.6 Ox +0.4 Red	Δ 2 = 0.6 Ox -0.6 Red	0.6 $\Delta_{(Phase)}$
Step 3 = 0.4 Ox +0.6 Red	Δ 3 = 0.4 Ox -0.4 Red	0.4 $\Delta_{(Phase)}$
Step 4 = 0.2 Ox +0.8 Red	Δ 4 = 0.2 Ox -0.2 Red	0.2 $\Delta_{(Phase)}$
End (5) = 0.0 Ox +1.0 Red	$\Delta_{(Phase)}$ = 0.0 Ox -0.0 Red	0

For a difference spectrum of amplitude 0.6, add 0.6 Ox and subtract 0.6 Red from the ending population of 0.0 Ox and 1.0 Red to yield populations of OX=0.6, Red=0.4.

Start = 0.8 Ox + 0.2 Red	Δ Start=0.8 Ox - 0.8 Red	$\Delta_{(Phase)}$
Step 1 = 0.6 Ox +0.4 Red	Δ 1 = 0.6 Ox - 0.6 Red	0.75 $\Delta_{(Phase)}$
Step 2 = 0.4 Ox +0.6 Red	Δ 2 = 0.4 Ox - 0.4 Red	0.5 $\Delta_{(Phase)}$
Step 3 = 0.2 Ox +0.8 Red	Δ 3 = 0.2 Ox - 0.2 Red	0.25 $\Delta_{(Phase)}$
End (4) = 0.0 Ox +1.0 Red	$\Delta_{(Phase)}$ = 0.0 Ox - 0.0 Red	0.0

For a difference spectrum of amplitude 0.5, add 0.4 Ox and subtract 0.4 Red from the ending population of 0.0 Ox and 1.0 Red to yield populations of OX=0.4, Red=0.6.

Scheme 1.

Figures

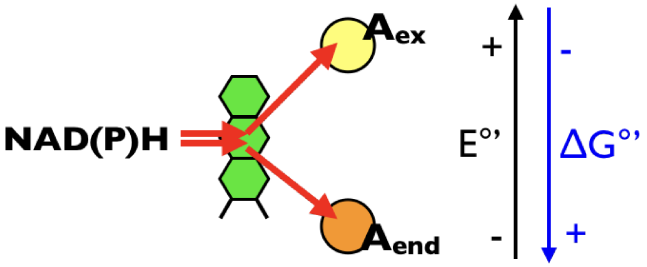

Figure 1.

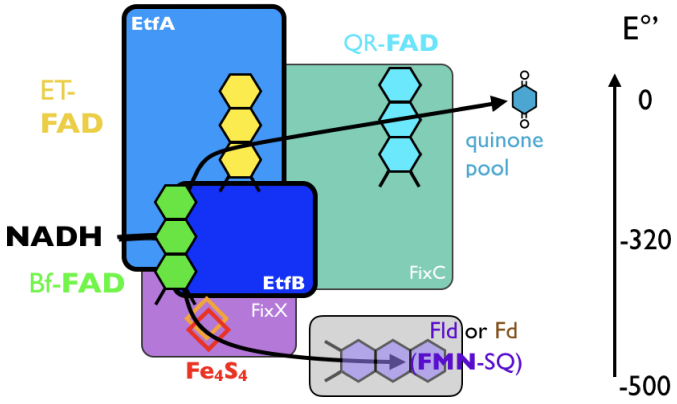

Figure 2.

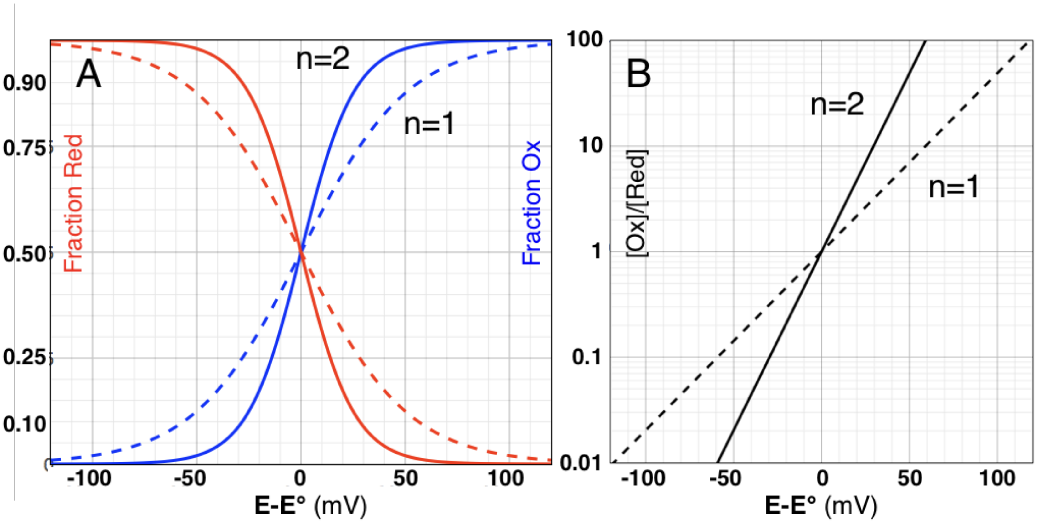

Figure 3.

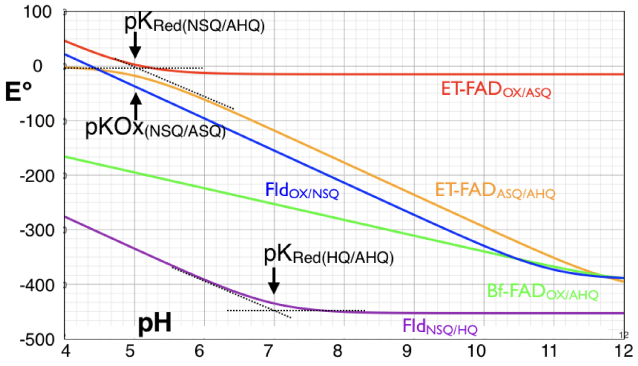

Figure 4.

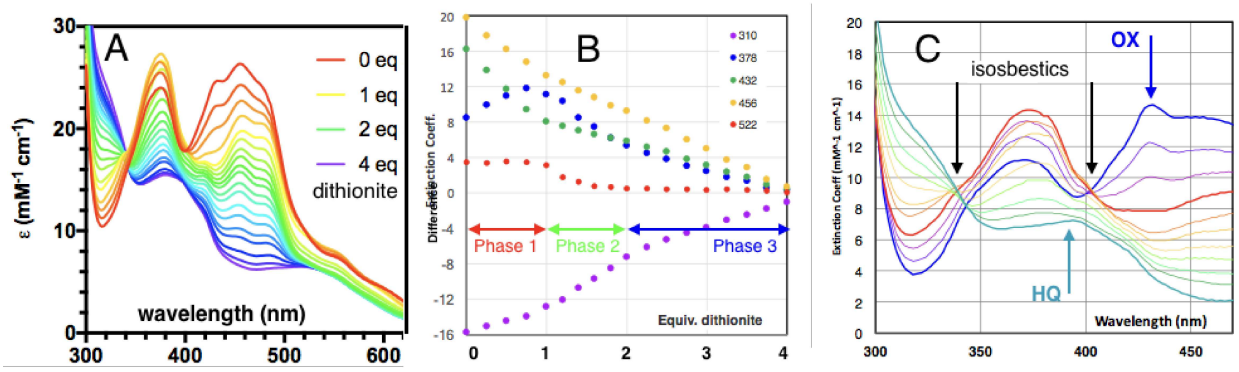

Figure 5.

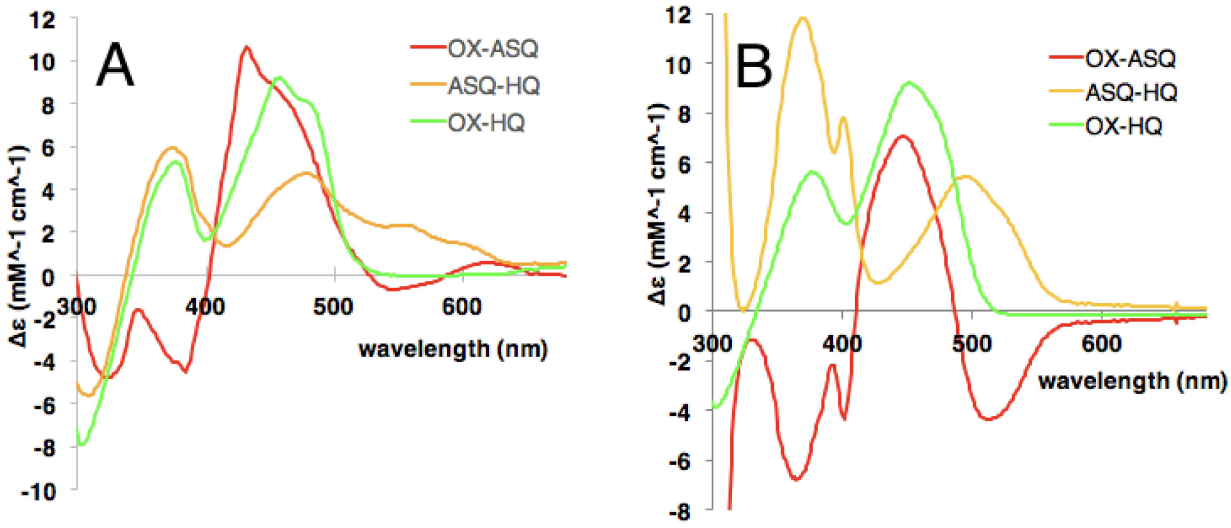

Figure 6.

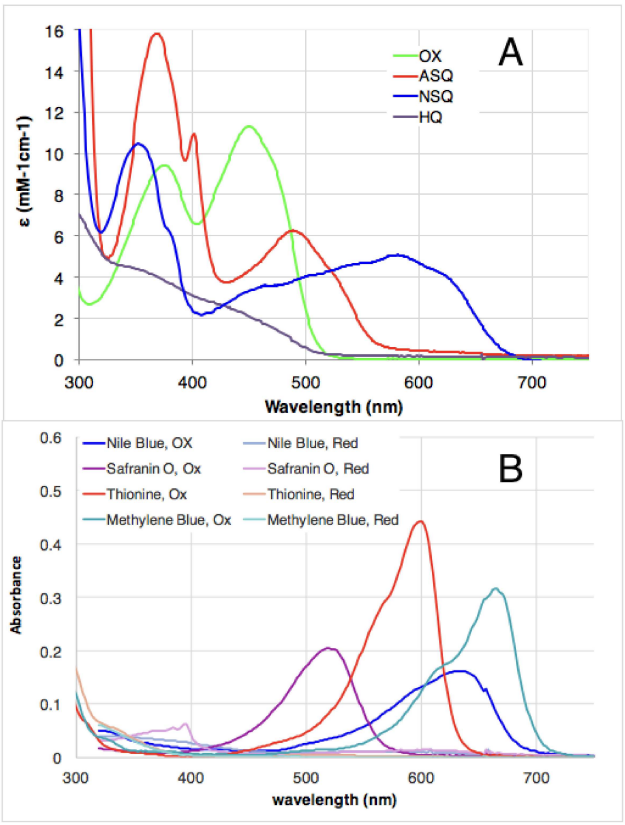

Figure 7.

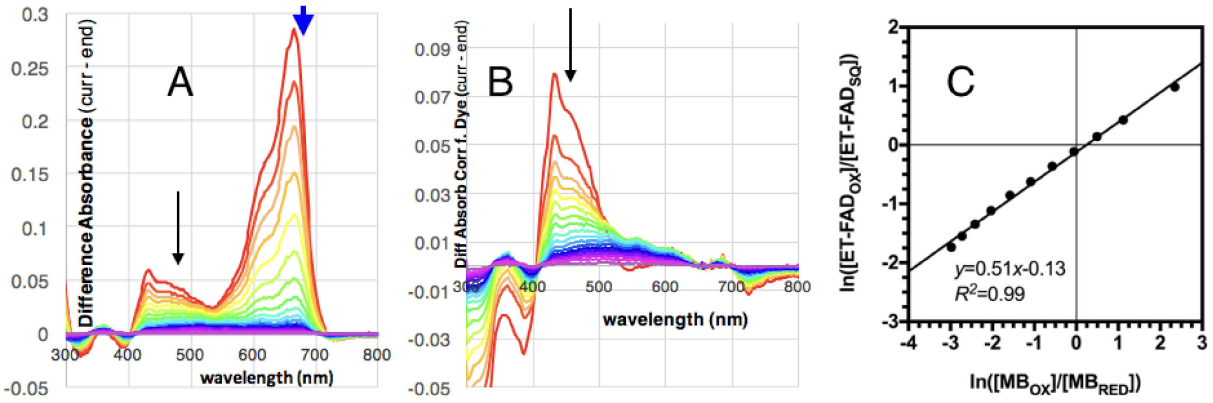

Figure 8.

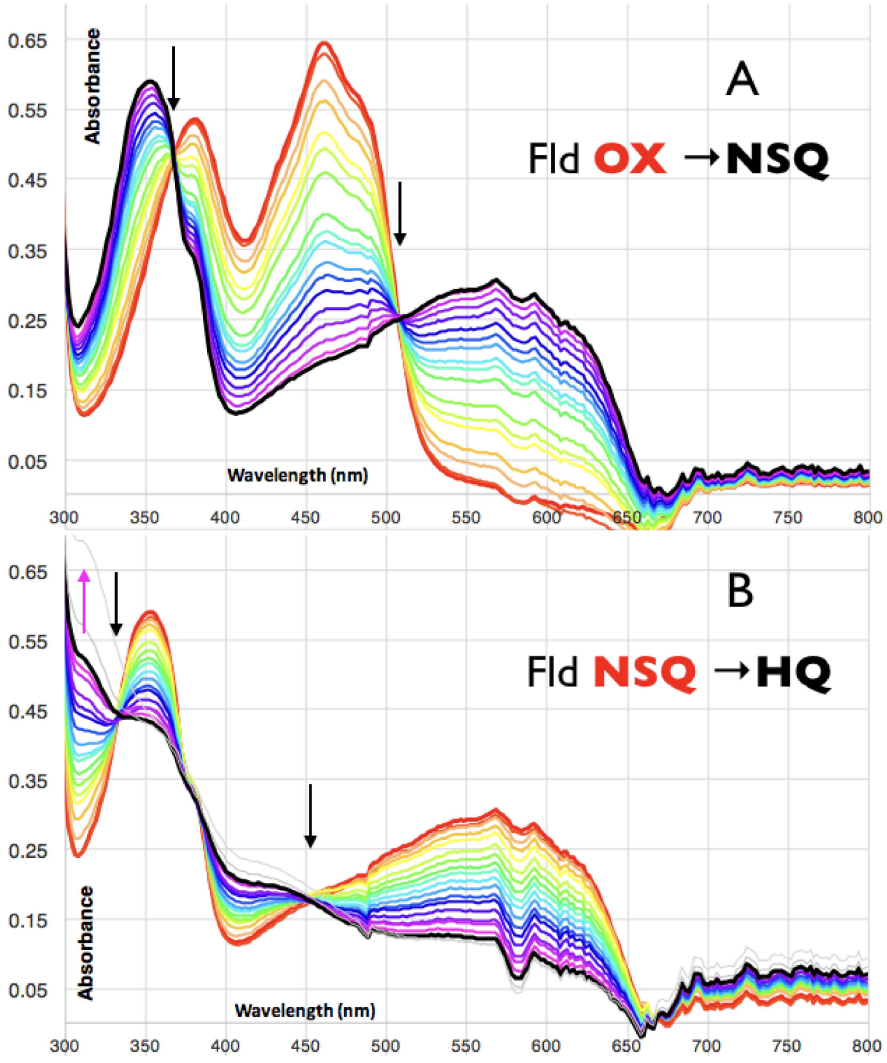
A
Fld OX →NSQ
Absorbance
Wavelength (nm)
B
Fld NSQ →HQ
Absorbance
Wavelength (nm)

Figure 9.

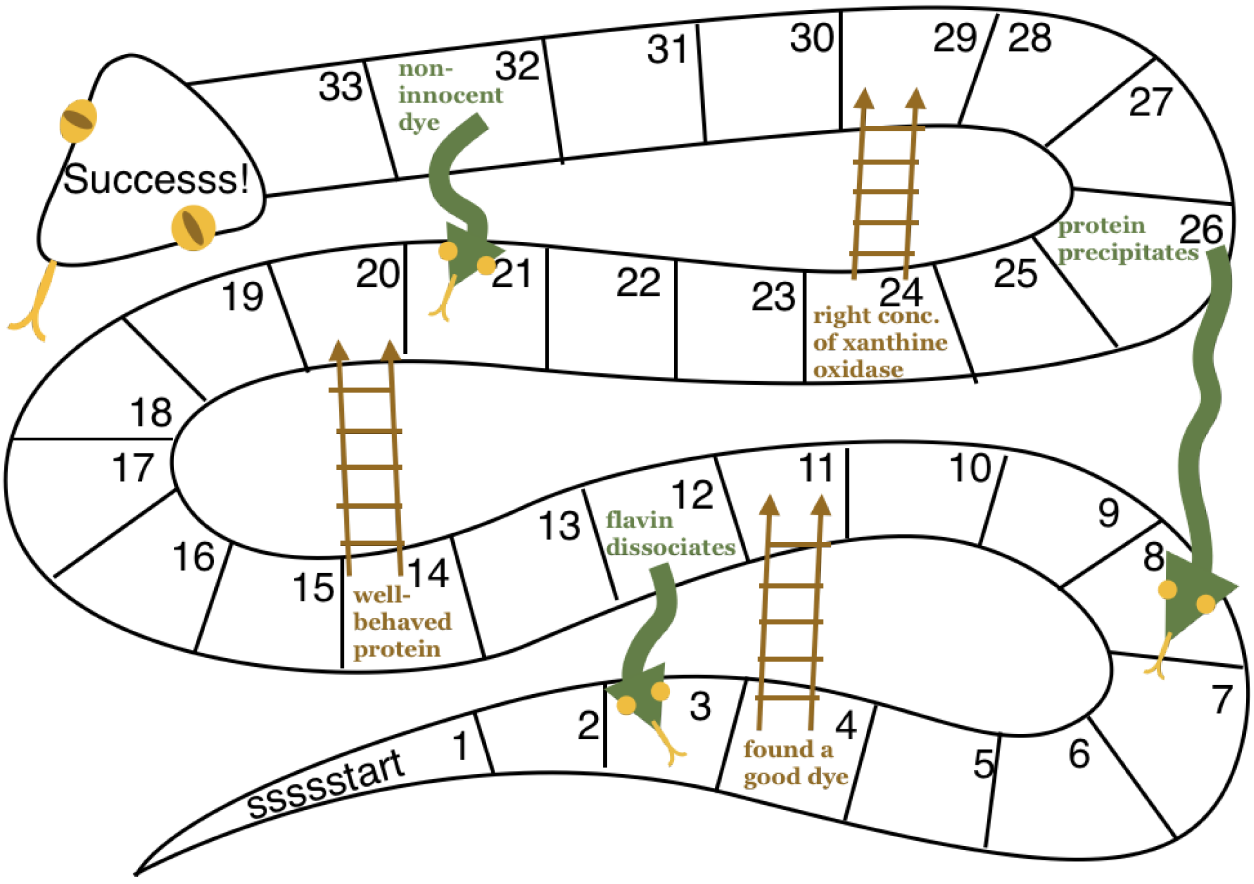
Successs!
33
non-
innocent
dye
32
31
30
29
28
27
protein
precipitates
26
25
24
right conc.
of xanthine
oxidase
23
22
21
20
19
18
17
16
15
well-
behaved
protein
14
13
flavin
dissociates
12
11
10
9
8
7
6
5
found a
good dye
4
3
2
sssssstart
1

Figure 10